NUMERICAL SIMULATION AND EXPERIMENT OF SPINNING FORMING OF HIGH STRENGTH ALUMINUM ALLOY TUBES

Zhang JIAN[1], Zhao SHUANG* [1], Lu FENGSHENG[2], Zhang LEI[2], Guo CE-AN[1]

Numerical simulation and experiments were carried out on tubes made of 2A12 high strength aluminum alloy in this paper. The DEFORM finite element (FE) software was used to analyze the process of power spinning. Then, the FE law of spinning forming was verified by experiments. The results showed that a number of factors, including the thinning rate, roller fillet radius, roller radius and feed rate, affect the quality of spinning forming, and the optimum simulation parameters were obtained. Compared with the experimental results, the error rate was 3.7% when the thinning rate was less than 15%, spinning roller radius was 180 mm and fillet radius was 20 mm.

Keywords: Power Spinning, Thinning Rate, Fillet Roller Radius, Roller Radius, Feed Rate, Finite Element

Introduction

Spinning is a common process of local deformation. The workpiece produced by the method of Power spinning with high strength, high utilization of materials and simple process [1]. Due to different materials on the roller workpiece parameters of the different requirements in the spinning experiment, defects which include interlayer, crack, inclusions and loose appear frequently inside of the blank. Scar, processing traces, cracks, burrs and etc. appear on the surface of outside at the same time [2]. A large number of researchers have been found the optimum spinning forming parameters to predict the defects of different spinning workpiece through theoretical analysis and experimental results [3-10]. It is difficult to satisfy the development of science and technology from the view of economy and time simply by using theoretical knowledge and multiple experiments. It is effective to predict the defects by using the combination of theoretical knowledge, computer simulation and experimental method. It has been found that the workpiece stress and strain distribution, deformation mechanism

[1] School of Equipment Engineering, Shenyang Ligong University, Shenyang 110159, Liaoning China; e-mail: zbgc2003@aliyun.com; *544383414@qq.com; 373055507@qq.com

[2] North Huaan Industrial Group Co., Ltd., Qiqihaer, 161046, China; e-mail: 18603627189@163.com; hzl560@163.com

and forming defects of spinning forming workpiece were obtained by a large number of researchers through the FE analysis and experimental results [11-14].

High-strength aluminum alloy has the strict requirements of the parameters for spinning forming. It is difficult to obtain the optimum parameters by experimental methods. This paper presents the optimum parameters of roller through simulation and experiments. First, the numerical simulation of 2A12 aluminum alloy tubes performed by multiple spinning. Then, the defects were predicted by changing the parameters of roller. Finally, the optimum parameters were obtained by combining with experiments. The software DEFORM were used in this paper.

1. Experimental Scheme and the FE

1.1 Experimental Scheme

The material of the blank is 2A12 aluminum alloy. The blank is processed by the method of treating the hot piercing into a prefabricated material. This prefabricated material is homogeneous and free defects. It meets the requirements of spinning. Yield strength of these material was around 390-400MPa. Chemical composition as shown in Table 1

Table 1

Chemical composition of 2A12 aluminum alloy (Mass fraction %)

Al	Si	Cu	Mg	Zn	Mn	Ti	Ni	Fe
Margin	0.50	4.0	1.47	0.30	0.5	0.15	0.40	0.43

Fig. 1 is a schematic diagram of forward spinning. The direction of the arrow is the metal flow direction.

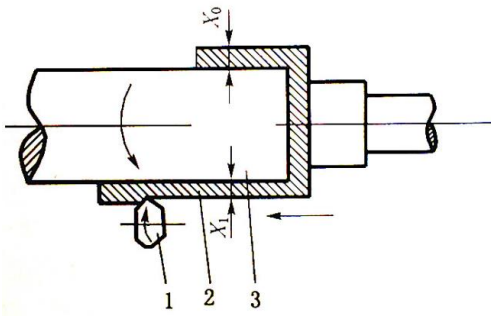

Fig. 1 Schematic diagram of forward spinning

1.2 FE modeling

Components can be drawn by using Solidworks. Then assembly drawing can be imported into DEFORM. Blank is made of elastoplastic material. By using DEFORM to automatically divide mesh function into blank mesh. To ensure accuracy, grid size should be choosing with small calculation criteria. The mandrel, the roller and the top block are rigid. The positive spin FE model of 2A12 aluminum cylinder can be shown in Fig. 2. The roller, the blank and mandrel are including.

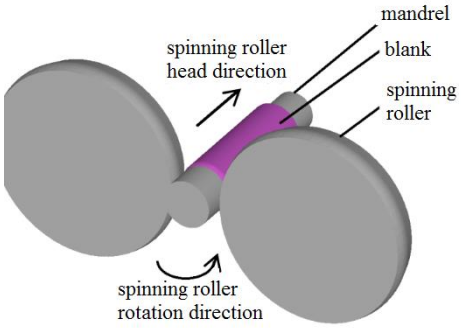

Fig. 2 FE modeling

2. Analyses and Discussion

2.1 Thinning Rate of the Roller

The range of the thinning rate is generally selected from 5 to 35% according to the material and multi-pass spinning. The process and deformation characteristics of large-scale cylindrical parts are different under different conditions of thinning rate. In this paper, thinning rate of 15%, 20%, 25% and 30% is selected for FE analysis, the stress nephogram and maximum equivalent stress curves can be shown as in Fig. 3 and 4.

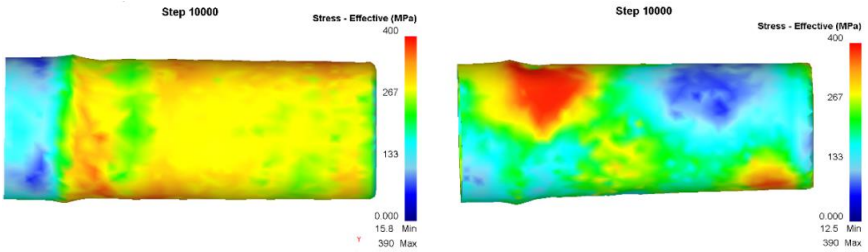

(a)15% (b)20%

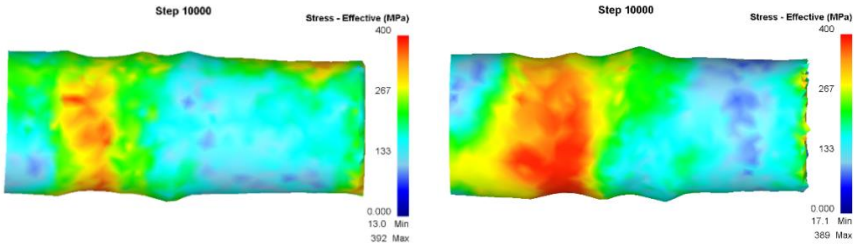

(c)25% (d)30%

Fig. 3 Stress nephogram with thinning rate of 15%, 20%, 25% and 30%

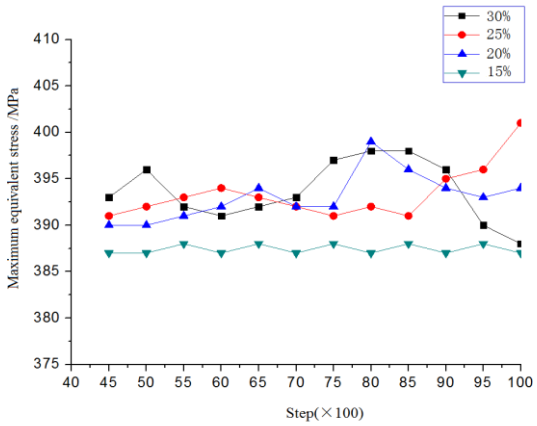

Fig. 4 Maximum equivalent stress curves with thinning rate of 15%, 20%, 25% and 30%

When the thinning rate was 30%, burrs and cracks appeared at the starting portion of the workpiece. Uplift phenomenon appeared at the middle part of the workpiece. The stress distribution of the workpiece was not uniform after spinning. A significant increase appeared in the middle part of the maximum equivalent stress. The maximum equivalent stress was greater than 400MPa; when the thinning rate was 25%, the burr and crack of the workpiece were reduced and the middle part was slightly increased. The stress distribution of the workpiece was not uniform after spinning. A slight increase appeared in the middle part of the maximum equivalent stress. The maximum equivalent stress was greater than 400MPa; when the thinning rate was 20%, Obvious uplift phenomenon did not appeare on the surface of the workpiece. The stress distribution of the workpiece was not uniform after spinning. A slight increase appeared in the middle part of the maximum equivalent stress. The maximum equivalent stress was greater than 400MPa; when the thinning rate was 15%, the workpiece surface did not appear burrs, cracks and uplift phenomenon. The stress distribution of the workpiece was uniform after spinning. The maximum equivalent stress distribution did not appear floating. The maximum equivalent stress was less than 400MPa. Radial stress and axial stress of the workpiece increased significantly under high thinning rate because the contact surface of the roller and the workpiece raised. The starting

portion of the workpiece appeared burrs, cracks and so on. The material flow increased. Then accumulation appeared in the middle part of the workpiece. When the material reached a certain limit of accumulation, maximum value of the radial stress and axial stress, Uplift, fracture and other defects appeared on the surface of the workpiece. Simulation results show no fracture on the surface when thinning rate of the roller less than 15% and maximum equivalent stress under 400MPa.

2.2 Fillet roller radius

Fillet roller radius was selected between 5 ~ 25mm according to different material. With the increase of the material thickness, the angle of the roller can be increased appropriately. With the increase of the blank thickness, fillet roller radius can be reduced. The spinning process and deformation characteristics of large cylindrical parts are different under the condition of different rounded corners. In this paper, fillet roller radius was chosen 8mm, 12mm, 16mm, 20mm for FE analysis, the stress nephogram and maximum equivalent stress curves can be shown as in Fig. 5 and 6.

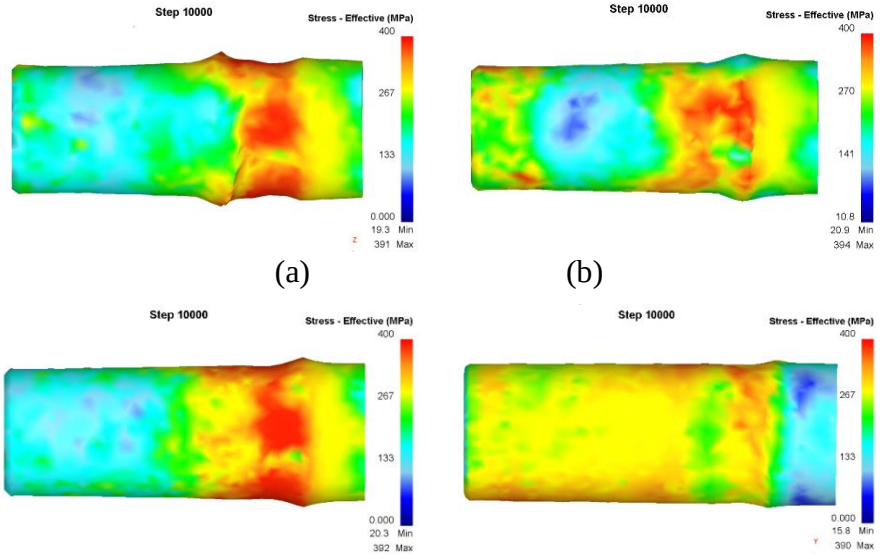

Fig.5 Stress nephogram with Fillet roller radius value of 8mm, 12mm, 16mm and 20mm

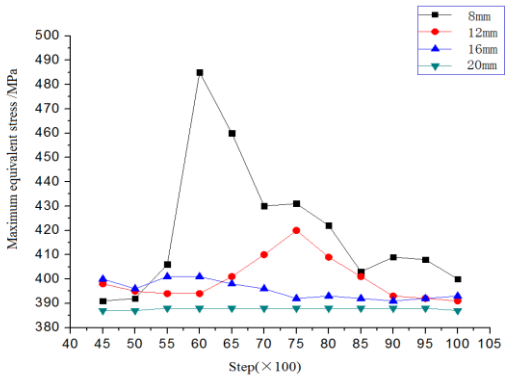

Fig.6 Maximum equivalent stress curves with fillet roller radius value of 8mm, 12mm, 16mm and 20mm

Fig. 5 and 6 shows that when fillet roller radius was around 8-12mm, burrs, cracks and uplift phenomenon appeared on the surface of the workpiece. The stress distribution of the workpiece was not uniform after spinning. A significant increase appeared in the middle part of the maximum equivalent stress. The maximum equivalent stress was greater than 400MPa; when fillet roller radius was 16mm, no burr, cracks and uplift phenomenon appeared on the surface of the workpiece. The stress distribution of the workpiece was not uniform after spinning. A slight increase appeared in the middle part of the maximum equivalent stress. The maximum equivalent stress was greater than 400MPa; when fillet roller radius was 20, no burr, cracks and obvious uplift phenomenon appeared on the surface of the workpiece. The stress distribution of the workpiece was uniform after spinning. The maximum equivalent stress was less than 400MPa. This was because when the roller angle was small, the radial force increased. The axial force and tangential force decreased. The radial stress of the contact point between blank and roller was too large. Material has a certain plasticity which caused burr, cracks and uplift phenomenon. When fillet roller radius and the spinning overlap increased, also the roller forward direction and metal flow direction contact gently, the workpiece surface was flat. However, with the roller and the blank contact area raised, part of the end of the workpiece stayed instability. The election pressure increased which result in the blank to withstand too much tension. And finally, the billet was fractured.

Simulation results show no fracture on the surface when fillet roller radius around 20mm and maximum equivalent stress under 400MPa.

2.3 Roller Radius

The spinning process and deformation characteristics of large cylindrical parts were different under the condition of different roller radius. With the increase of the material strength, the roller angle was increased. Deformation

characteristics were different. In this paper, roller radius was chosen 90mm, 120mm, 150mm, 180mm for FE analysi, the stress nephogram and maximum equivalent stress curves can be shown as in Fig. 7 and 8.

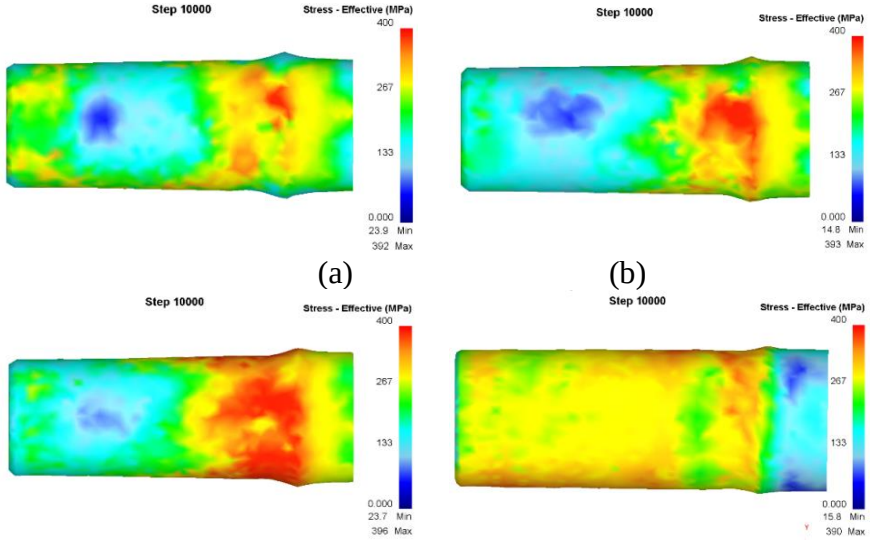

Fig 7 Stress nephogram with roller radius value of 90mm, 120mm, 150mm and 180mm

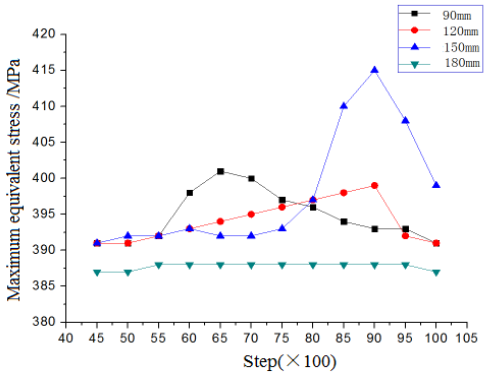

Fig 8 Maximum equivalent stress curves with fillet roller radius value of 90mm, 120mm, 150mm and 180mm

Figs. 7 and 8 shows that when roller radius was 90mm, the stress distribution of the workpiece was not uniform after spinning. A significant increase appeared in the middle part of the maximum equivalent stress. The maximum equivalent stress was greater than 400MPa; when roller radius was 120mm, the stress distribution of the workpiece was not uniform after spinning. The maximum equivalent stress raised as the number of spinning steps increased. The maximum equivalent stress was greater than 400MPa; when roller radius was 150mm, the stress distribution of the workpiece was uniform after spinning. The maximum equivalent stress did not appear to float. With the increase of the diameter of the roller, the contact between the roller and the workpiece surface

increased. The contact area per unit time raised with the workpiece. The election pressure increased slightly and the pressure distribution on the surface of the workpiece decreased. Roller forward direction and the workpiece metal flow direction contact gently. The surface was flat.

2.4 Roller feed rate

The optional feedrate was in the range of 0.5 to 3 according to the feed rate and the material. The increase of the roller feed rate can improve the production efficiency. However, excessive feed rates cause defects in the actual production. In this paper, roller feed rate was chosen 0.8mm/r, 0.9mm/r, 1.0mm/r, 1.1mm/r for FE analysis according to different material, roller feed rate, spinning process and deformation characteristics. The stress nephogram and maximum equivalent stress curves can be seen as in Fig. 9 and 10.

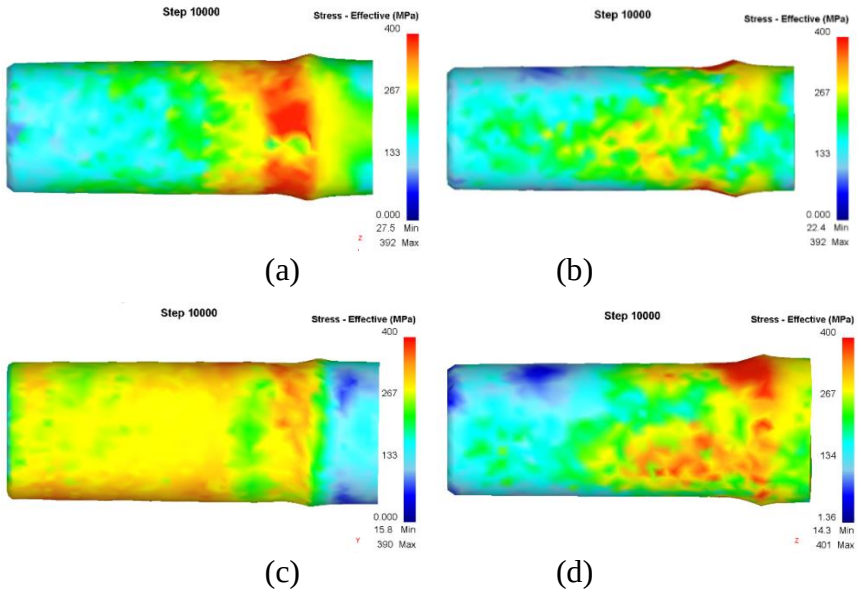

Fig. 9 Stress nephogram with roller feed rate of 0.8mm/r, 0.9mm/r, 1.0mm/r, 1.1mm/r

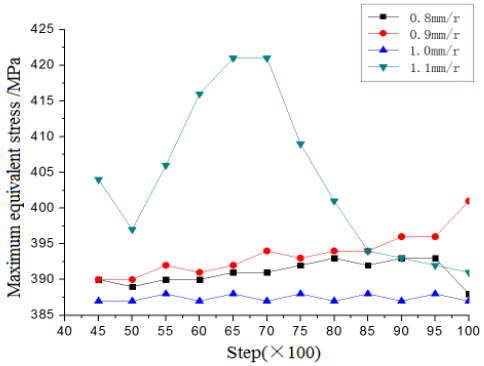

Fig. 10 Maximum equivalent stress curves with roller feed rate of 0.8mm/r, 0.9mm/r, 1.0mm/r, 1.1mm/r

Figs. 9 and 10 shows that when roller feed rate was around 0.8-0.9mm/r, the stress distribution of the workpiece was not uniform after spinning. The maximum equivalent stress had a greater float and was greater than 400MPa; when roller feed rate was 1.0mm/r, the stress distribution of the workpiece was uniform after spinning. The maximum equivalent stress did not appear to float. The maximum equivalent stress was less than 400MPa; when roller feed rate was 1.1mm/r, the stress distribution of the workpiece was not uniform after spinning. The maximum equivalent stress had a greater float and was greater than 400MPa. When feed rate was small, the former one was overlapped with the next one. Due to the flow of materials and extrusion, making the process of spinning parts of the workpiece stress was too large. The phenomenon of sandwich emerged. As the feed rate increased, the coincidence zone became smaller and reached the best value of a stress distribution. If the feed rate is too large, the axial and circumferential metal flows greater. Deformation of the region led to greater flow of metal parts of the workpiece caused by excessive stress. It caused uplift phenomenon. Simulation results show no fracture on the surface when roller feed rate was around 1mm/r and maximum equivalent stress under 400MPa.

3. Experimental Results

Figs. 11 and 12 show the simulation results of the workpiece before modification. Before the improvement, the workpiece passes through a spinning pass. The results show that thinning rate was 28%, fillet roller radius was 8mm, feed rate was 1.3mm/r and roller radius was 150mm.

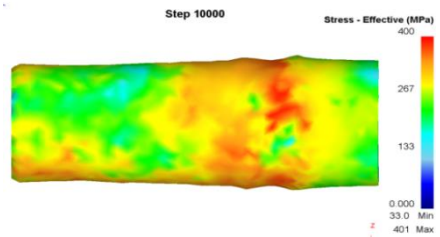

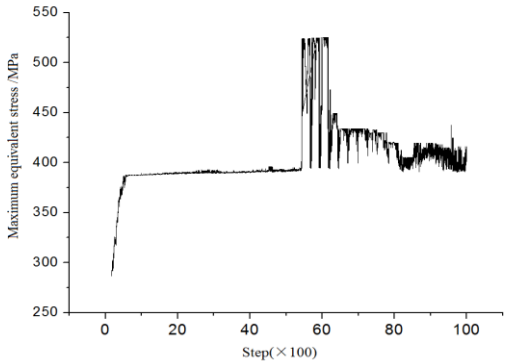

Fig. 11 Simulation results of the workpiece before modification
Fig. 12 Maximum equivalent stress of the workpiece before modification

As it can be seen from Figs. 11 and 12, the middle part of the workpiece was not smooth after spinning. The maximum equivalent stress experienced a significant. Burrs, cracks and uplift phenomenon appeared on the surface of the workpiece. Defects such as material Stacking appeared in the end of the workpiece.

Fig. 13 shows the workpiece before modification. As can be seen in Fig. 13, scales and cracks appeared on the surface of the workpiece after spinning. Defects such as material Stacking appeared in the end of the workpiece which result fracture. Experimental results were carried out to verify simulation.

Simulation results presented that optimal step of mutil-pass spinning for blank was three. Thinning rate should less than 15%. The optimal thinning rates were 12%, 10% and 9%. Fillet roller radius was 20mm. Roller diameter was 180mm. Roller feed rate was 1mm/r. The stress nephogram and maximum equivalent stress curves of the workpiece after three times spinning and thinning as seen in Fig. 14 and 15.

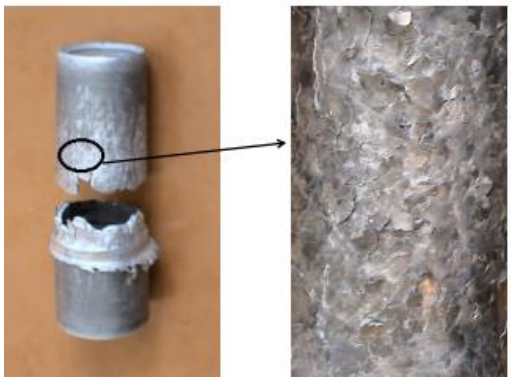

Fig. 13 Workpiece before modification

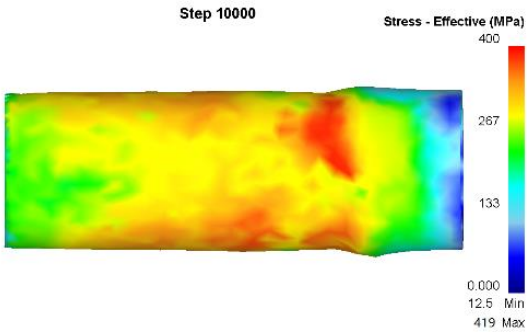

Fig. 14 The stress nephogram of the workpiece after three times spinning and thinning

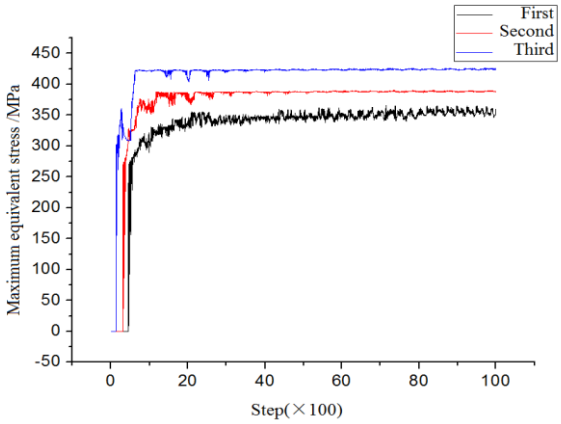

Fig. 15 Equivalent stress curves of the workpiece after three times spinning and thinning

The stress distribution of the workpiece was uniform after three times spinning. The maximum equivalent stress had a certain floating after the first spinning. The stress tended to be stable around 340 ~ 360MPa. The maximum equivalent stress had a slight floating after the second spinning. The stress tended to be stable around 375 ~ 390MPa. The maximum equivalent stress also had a slight floating after the third spinning. The stress tended to be stable around 410 ~

420MPa.

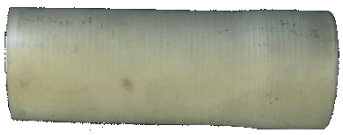

Fig 16 Workpiece after three times spinning

Fig. 16 shows the workpiece after three times spinning. As it can be seen from Fig. 16, no defects on the surface of the workpiece. Simulation results show that thickness of three times thinning was 2mm while experimental results show thickness was 1.926mm. The error was 3.7%. Experimental results were carried out to verify simulation.

4. Conclusions

(1) The FE software DEFORM was used to establish the three-dimensional FE model of the tubes made of 2A12 high strength hard aluminum alloy, and the spinning forming process was successfully simulated, which can lay a good foundation for the further study of spinning parts.

(2) By using the FE software DEFORM, the influence of the roller parameters on the forward spinning tube made of 2A12 high strength hard aluminum alloy was obtained, and the optimum parameters are as follows: the thinning rate is below 15%; the radius of the roller fillet is 20mm; the roller radius is 180mm; and the feed rate is 1mm/r.

(3) Through the comparison of the simulated results and the experimental results, the stress and strain distribution laws were analyzed to predict the defects, which can provide a reliable basis for the rational selection and optimization of the spinning process parameters.

R E F E R E N C E S

[1]. *Hayama M, Kudo H.* Analysis of diametrical growth and working forces in tube spinning, J. Sci. Bulletin of Japan Society of Mechanical Engineers. 22 (1979) 776-784.

[2]. *Davidson M J, Balasubramanian K, Tagore G R N.* An experimental study on the quality of flow-formed AA6061 tubes, J. Sci. Journal of Materials Processing Technology. 203 (2008) 321−325.

[3]. *M. Kuss, B. Buchmayr.* Damage minimised ball spinning process design, J. Sci. Journal of Materials Processing Technology. 234 (2016) 10-17.

[4]. *L. Kwiatkowski, A.E. Tekkaya, M. Kleiner.* Fundamentals for Controlling Thickness and Surface Quality During Dieless Necking-in of Tubes by Spinning, J. Sci. CIRP Annals-Manufacturing Technology. 62 (2013) 299-302.
[5]. *N. Akkus, M Kawahara.* An Experimental and Analytical Study on Dome Forming of Seamless Al Tube by Spinning Process, J. Sci. Journal of Materials Processing Technology. 173 (2006) 145-150.
[6]. *Sebastian Hartel, Robert Laue.* An Optimization Approach in Non-circular Spinning, J. Sci. Journal of Materials Processing Technology. 229 (2016) 417-430.
[7]. *Xiaohui Cui, Jianhua Mo, Jianjun Li et al.* Large-scale Sheet Deformation Process by Electromagnetic Incremental Forming Combined with Stretch Forming, J. Sci. Journal of Materials Processing Technology. 237 (2016) 139-154.
[8]. *Gangfeng Xiao, Qinxiang Xia, Xiuquan Cheng et al.* Metal Flow Model of Cylindrical Parts by Counter-roller spinning, J. Sci. Procedia Engineering. 81 (2014) 2397-2402.
[9]. *Mohebbi M S, Akbarzadeh A.* Experimental study and FEM analysis of redundant strains in flow forming of tubes, J. Sci. Journal of Materials Processing Technology. 210 (2010) 389-395.
[10]. *Wong C C, Danno A, Tong K K et al.* Cold rotary forming of thin-wall component from flat-disc blank, J. Sci. Journal of materials processing technology. 208 (2008) 53-62.
[11]. *XIA Qinxiang, YANG Minghui, HU Xing, et al.* Numerical Simulation and Experimentation Cup-Shaped Thin-Walled Inner Rectangular Gear Formed by Spinning, J. EI. Journal of Mechanical Engineering. 42(12) (2006) 192-196.
[12]. *XIA Qinxiang, SHANG Yue, ZHANG Shuaibin et al.* Numerical Simulation and Experimental Investigation on the Multi-pass Neck-spinning of Non-axisymmetric Oblique Tube, J. EI. Journal of Mechanical Engineering. 44(8) (2008) 78-84.
[13]. *XIA Qinxiang, ZHANG Saijun, LIANG Baixiang et al.* Analysis on the Spinning Forces for 3D Non-axisymmetrical Thin-walled Offset Tubes. Journal of Mechanical Engineering, 2005, 41(10): 200-204.